AFRL-RV-PS-
TR-2010-1112

DEVELOPMENT OF A RESEARCH PLAN TO MINIMIZE THERMAL CONDUCTIVITY IN LOW TEMPERATURE THERMOELECTRIC MATERIALS

Jennifer R. Lukes

University of Pennsylvania
220 S. 33rd Street
Philadelphia, Pennsylvania 19104-6315

3 December 2010

Final Report

AIR FORCE RESEARCH LABORATORY
Space Vehicles Directorate
3550 Aberdeen Ave SE
AIR FORCE MATERIEL COMMAND
KIRTLAND AIR FORCE BASE, NM 87117-5776

DTIC COPY

NOTICE AND SIGNATURE PAGE

This report was cleared for public release by the Air Force Research Laboratory RV Public Affairs Office and is available to the general public, including foreign nationals. Copies may be obtained from the Defense Technical Information Center (DTIC) (http://www.dtic.mil).

AFRL-RV-PS-TR-2010-1112 HAS BEEN REVIEWED AND IS APPROVED FOR PUBLICATION IN ACCORDANCE WITH ASSIGNED DISTRIBUTION STATEMENT.

//SIGNED//
CLAY MAYBERRY
Program Manager

//SIGNED//
WILLIAM A. SCHUM, Lt Col, USAF
Deputy Chief, Spacecraft Technology Division
Space Vehicles Directorate

REPORT DOCUMENTATION PAGE

Form Approved
OMB No. 0704-0188

1. REPORT DATE *(DD-MM-YY)*	**2. REPORT TYPE**	**3. DATES COVERED** *(From - To)*
03-12-10	Final Report	21-09-09 to 21-09-10

4. TITLE AND SUBTITLE
Development of a Research Plan to Minimize Thermal Conductivity in Low Temperature Thermoelectric Materials

5a. CONTRACT NUMBER
FA9453-09-1-0001

5b. GRANT NUMBER

5c. PROGRAM ELEMENT NUMBER
62601F

6. AUTHOR(S)

Jennifer R. Lukes

5d. PROJECT NUMBER
8809

5e. TASK NUMBER

5f. WORK UNIT NUMBER
837659

7. PERFORMING ORGANIZATION NAME(S) AND ADDRESS(ES)

University of Pennsylvania
220 S. 33rd Street
Philadelphia, Pennsylvania 19104-6315

8. PERFORMING ORGANIZATION REPORT

9. SPONSORING / MONITORING AGENCY NAME(S) AND ADDRESS(ES)
Air Force Research Laboratory
Space Vehicles Directorate
3550 Aberdeen Ave., SE
Kirtland AFB, NM 87117-5776

10. SPONSOR/MONITOR'S ACRONYM(S)
AFRL/RVSE

11. SPONSOR/MONITOR'S REPORT NUMBER(S)
AFRL-RV-PS-TR-2010-1112

12. DISTRIBUTION / AVAILABILITY STATEMENT
Approved for public release; distribution is unlimited. (377ABW-2010-1744, dtd 15 Dec 2010)

13. SUPPLEMENTARY NOTES

14. ABSTRACT
Minimizing thermal conductivity in thermoelectric materials is critical for the operation of infrared sensors at 10K. Various nanostructures including superlattices, ball milled nanocomposites, and rough nanowires have all shown promise for significant low-temperature thermal conductivity reduction, with rough nanowires demonstrating 4 order of magnitude reduction as compared to bulk. Here computer simulations are used to investigate two factors potentially responsible for thermal conductivity reduction: confinement effects on phonon dispersion and roughness effects on phonon transmission. Increased understanding of the mechanisms responsible for thermal conductivity reduction will potentially enable thermoelectric material nanostructures to be tuned to maximize ZT.

15. SUBJECT TERMS
Thermal Conductivity; Temperature Thermoelectric Materials; Nano Structures

16. SECURITY CLASSIFICATION OF:			**17. LIMITATION OF ABSTRACT**	**18. NUMBER OF PAGES**	**19a. NAME OF RESPONSIBLE PERSON**
a. REPORT	**b. ABSTRACT**	**c. THIS PAGE**			**19b. TELEPHONE NUMBER** *(include area code)*
Unclassified	Unclassified	Unclassified	Unlimited	28	Clay Mayberry

Standard Form 298 (Rev. 8-98)
Prescribed by ANSI Std. 239.18

(This page intentionally left blank)

TABLE OF CONTENTS

LIST OF FIGURES

GLOSSARY

A	normalization constant
A modes	antisymmetric Lamb modes
A_c	nanostructure cross sectional area
a	silicon lattice constant
Bi_2Te_3/Sb_2Te	bismuth telluride / antimony telluride
$\bar{C}$	stiffness matrix
ErAs	erbium arsenide
f	phonon distribution function
FDTD	finite difference time domain simulation
h	waveguide dimension
InGaAs	indium gallium arsenide
j	atom index
k	wave vector
k*	dimensionless wave vector
k_x	x-direction wave vector
L	nanostructure length
MD	molecular dynamics simulation
N_a	number of atoms
N_b	number of phonon modes (branches)
n_{max}	maximum number of phonons
S	Seebeck coefficient
S modes	symmetric Lamb modes

SH modes	shear horizontal modes
Si	silicon
SiGe	silicon germanium
SPW	superposition of partial waves method
T	temperature
t	time
t_{center}	time of maximum wavepacket displacement
$\dot{u}_{j,\alpha}$	j^{th} atom's velocity component in the α direction
v	phonon velocity
x_j	j^{th} atom's x-position
$x_{j,0}$	j^{th} atom's equilibrium x-position
U	wavepacket amplitude
V	shear wave velocity
ZT	thermoelectric figure of merit
α	Cartesian component
Φ	spectral energy density
η	wavepacket temporal decay parameter
κ	thermal conductivity
λ_{dom}	dominant wavelength
ω	phonon angular frequency
σ	electrical conductivity
$\mathcal{T}$	phonon transmission function

τ	phonon lifetime
τ_0	integration time period for spectral energy density
$< >$	average
*	dimensionless

1.0 INTRODUCTION

1.1 Motivation

Cooling of infrared sensors to very low temperatures is essential for highly sensitive detection of long wavelength radiation in defense surveillance applications. Mechanical refrigeration approaches such as Stirling, reverse Brayton, and Joule-Thomson cycle coolers are frequently used to attain such temperatures {3}. Thermoelectric cooling with Peltier junctions offers a solid state, lightweight, high reliability alternative to these approaches, with the added benefit of no moving parts. However, the thermoelectric materials typically used in such applications are not yet competitive in terms of efficiency with existing mechanical cycles. To become competitive with other cooling technologies, an increase in the thermoelectric figure-of-merit ZT beyond that of the workhorse material Bi_2Te_3 is required. The figure-of-merit is defined as

$$ZT = S^2 \sigma T / k \quad (1)$$

where S is Seebeck coefficient, σ is electrical conductivity, and k is thermal conductivity.

1.2 Background

1.2.1 Low-Dimensional Materials for Reducing Thermal Conductivity

Low-dimensional materials, or materials with at least one nanoscale characteristic dimension, emerged in the 1990s as a potential route to increasing ZT dramatically. This large increase was theoretically predicted to arise from nanoscale confinement of electronic carriers, leading to an increase of the power factor $S^2 \sigma$, and from reduction of thermal conductivity {4}. Since then, a significant amount of research effort has been directed toward characterizing the thermoelectric properties of nanomaterials. The materials investigated have primarily been superlattices, but quantum dot superlattices, random quantum dot composites, compacted bulk composite materials with nanosized grains, and nanowires {4-5} have also been investigated. The evidence from these investigations is that thermal conductivity reduction in these nanoscale materials is the primary factor responsible for the observed increases in ZT {4}. For this reason there is much research interest in reducing the thermal conductivity of these materials in a controllable manner to optimize ZT.

1.2.2 Nanometer-Scale Dominant Phonon Wavelengths

Thermal conductivity reduction in nanoscale thermoelectric materials arises from the additional phonon scattering that occurs at nanomaterial interfaces. Phonons, which are the lattice vibrations that transport energy throughout a material, exist in a broad spectrum of wavelengths. At low temperatures, such as the ~10 K of interest in the cooling of infrared sensors, the phonons in a material follow the Planck distribution (Fig. 1). The peak of this distribution represents the wavelength (λ_{dom}) at which the maximum number of phonons (n_{max}) are present. Hence it is important to design materials that scatter phonons of wavelength λ_{dom}, and this is typically done when characteristic structural dimensions of these materials are roughly the same

size as this wavelength. At 10 K, λ_{dom} is of order 20 nm, so the structures should also be of this order of magnitude.

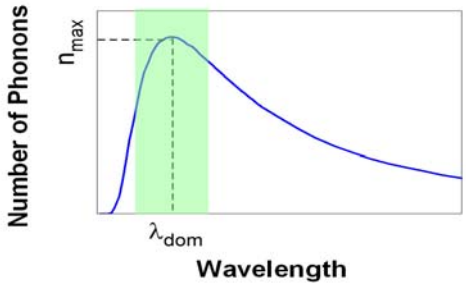

Figure 1: Planck Distribution of Phonon Wavelengths

1.2.3 Scattering at Multiple Length Scales for Thermal Conductivity Reduction

Recent research indicates that thermoelectric nanomaterials with *multiple* characteristic dimensions, rather than a single characteristic dimension of order λ_{dom}, can reduce thermal conductivity and thus increase ZT. For example, nanocrystalline materials (p-type Bi_2Te_3/Sb_2Te, n-type SiGe, and p-type SiGe) with grain sizes ranging from 5–50 nm show a ~20%-50% reduction in thermal conductivity below that of the bulk SiGe alloy used in space power missions at the lowest temperatures measured for these samples (~300-325 K) {6-8}. InGaAs alloy with embedded 1-4 nm ErAs particles crystalline demonstrates a ~35% reduction in thermal conductivity below InGaAs alloy without particles {9}. Most dramatically, *silicon nanowires with a range of diameters (20-300 nm) and surface roughnesses (1-5 nm) exhibit a* ***4 order of magnitude reduction in thermal conductivity*** *at the lowest temperatures measured* (25 K) {5}.

The reason for thermal conductivity reduction is not completely understood in materials with multiple nanostructure sizes {5}. The reduction is likely related to the increased scattering of phonons at a variety of different wavelengths by the presence of scatterers on multiple length scales. Figure 1 indicates that in order to scatter the most phonons, it may be most beneficial to for the different nanostructure dimensions to be focused in a small band centered on the dominant wavelength, and clear thermal conductivity reduction has been observed in materials with a moderately narrow range of characteristic sizes {6-8}. However, excellent results have also been achieved with widely divergent sizes spanning two orders of magnitude {5}. The optimal combination and range of nanostructure sizes to reduce thermal conductivity remains an open question.

1.2.4 Significance of Dispersion Relations

Two mechanisms thought to contribute to the low thermal conductivity observed in rough silicon nanowires at low temperature are the confinement effects on dispersion relations and the wire roughness effects on phonon transmission. Analysis of the sensitivity of these factors to nanostructure geometry will be important in uncovering clear structure-property relationships that will provide guidance for fabrication of other low thermal conductivity nanostructures.

Simply put, a dispersion relation is a plot of phonon frequency versus wavevector for all vibrational modes of a material or structure. Dispersion relations contain information on the phonon modes and velocities that is directly related to thermal conductivity through the expressions {10}

$$\kappa(T) = \frac{L}{A_c}\int_0^{\infty} \mathcal{T}(\omega)\frac{\hbar\omega}{2\pi}\frac{df}{dT}d\omega \tag{2}$$

and

$$\mathcal{T}(\omega) = N_b(\omega)\frac{\tau(\omega)\langle v(\omega)\rangle}{L} \ . \tag{3}$$

Equation (2) represents thermal conductivity as a function of temperature. The parameters in this expression are nanostructure length L, nanostructure cross sectional area A_c, phonon frequency ω, phonon distribution function f, and frequency dependent phonon transmission function for the nanostructure $\mathcal{T}(\omega)$. Phonon transmission function is computed following Equation (3), where $N_b(\omega)$, $\tau(\omega)$, and $\langle v(\omega)\rangle$ represent the number of modes, lifetime, and average velocity of phonons with frequency ω.

The specific parameters obtained from dispersion relations that are needed to calculate thermal conductivity are $N_b(\omega)$,and $v(\omega)$. These parameters can be calculated as follows. First, a frequency ω is chosen. The number of modes at that frequency can be calculated by counting the number of dispersion branches that intersect the horizontal line at frequency ω. The phonon group velocity can be determined from the slope of each branch; these values can be averaged over all branches to obtain $\langle v(\omega)\rangle$.

1.2.5 Significance of Phonon Transmission Functions

Phonon transmission functions represent the fraction of energy input to one end of the nanostructure that leaves the other end of the nanostructure. They can be calculated as in Equation (3) provided that the frequency dependence of phonon lifetimes is known. Although the functional form of phonon lifetime has been established for some phonon scattering processes in certain frequency ranges, there is no simple universal description of this phonon lifetime. As a result, $\tau(\omega)$ is often not well known and direct calculations of $\mathcal{T}(\omega)$ using Equation (3) are approximate at best. There are several alternative methods to calculate $\mathcal{T}(\omega)$ without using Equation (3) that can easily incorporate details of the nanostructure geometry.

2.0 OBJECTIVE

The objective of this work was to use computer simulations to investigate two factors potentially responsible for the low thermal conductivity observed in rough silicon nanowires at low

temperature: confinement effects on the phonon dispersion relation and wire roughness effects on phonon transmission. Although nanostructured materials of various configurations including superlattices, quantum dot superlattices, ball milled nanocomposites, and rough nanowires have shown encouraging results, this research focused on rough nanowires, as these have shown the greatest potential to date for reduction in thermal conductivity at low temperature (4 orders of magnitude lower than bulk silicon). An increased understanding of the mechanisms responsible for thermal conductivity reduction will potentially enable the optimal engineering of nanostructure configuration in a wide variety of low temperature thermoelectric materials in order to minimize thermal conductivity and maximize ZT.

3.0 METHODOLOGY

3.1 Overview

Simulations of silicon nanostructures of varying widths, geometries, and surface 'roughnesses' were performed using three different computational approaches: molecular dynamics simulations, finite difference time domain simulations, and the superposition of partial waves analytical method. Multiple approaches were used in order to self-validate the computations. Dispersion relations and transmission calculations were performed for the various nanostructure configurations.

3.2 Molecular Dynamics Simulation Method

3.2.1 Overview

Molecular dynamics (MD) simulation {11} is a computational technique that models materials at an atomic level of detail. Each atom is represented as a classical particle connected to other atoms in the system through 'springs' whose stiffnesses are governed by the interatomic potential interactions chosen for a given material. Figure 2 provides a schematic illustration of atoms (green particles) arranged into a crystalline structure. Each atom interacts with all its neighbors within a certain 'cutoff' distance, resulting in coupled dynamical motions of all particles in the system. Interatomic potential models for materials are determined by fitting parameters in the potential to experimental data and/or the results of ab initio quantum computations and there are often multiple potentials available for any given material that are optimized for specific physical properties of the material. Trajectories are computed for all atoms in the system using classical Newtonian mechanics. Forces are calculated from the negative derivative of the interatomic potential function and velocities and positions are calculated via numerical integration, most often using explicit numerical algorithms such as velocity Verlet or Gear integrators. A wide variety of information can be extracted from MD simulation data, including temperature, stress, energy, mechanical properties, thermal conductivity, and wave propagation phenomena.

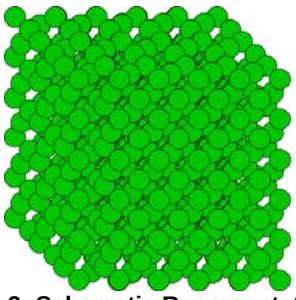

Figure 2: Schematic Representation of Crystalline Material in Molecular Dynamics

There are several advantages of MD for the present study. First, it is intrinsically capable of modeling wave transport phenomena such as interference and scattering. Other approaches that use continuum approximations can also model these phenomena, but are not capable of handling the atomic scale 'roughness' seen by waves of high wavenumber. Related to this, MD also handles dispersion effects arising from the discrete atomic nature of the system. Additionally, MD is capable of handling, qualitatively, nanoscale confinement effects on phonon dispersion relations. Other benefits of the technique are that it does not require input of adjustable specular scattering parameters, which are often unknown and typically neglect scattering variations present at different phonon frequencies, that it intrinsically captures the directions and magnitudes of the scattering of individual phonons, that it is not restricted to linearly elastic materials, and that it does not make assumptions about diffuse or specular scattering.

3.2.2 Calculation of Dispersion Relations with Molecular Dynamics

In these calculations the silicon atoms are set up in a diamond lattice configuration and simulations are performed for three different geometries: bulk, thin film ('nanoplate'), and wire geometries. The Stillinger-Weber interatomic potential model {12} is used in all simulations. The bulk geometry is studied in order to validate the MD simulation results against the numerical and experimental data of other groups. The thin film 'nanoplate' geometry, for cases of low frequency and wavenumber, can also be validated by comparing to continuum based calculation methods. Other thin film and nanowire cases studied here are not amenable to continuum treatment and atomistic approaches such as MD are required. For all cases the dispersion is calculated along the k_x ([100]) direction.

Figure 3 illustrates the computational setup for the three geometries. For all geometries the x-direction domain length is 300 unit cells (≈163nm). For the bulk simulations periodic boundary conditions are applied in all three directions. The periodic domain width in y- and z- directions is 4 unit cells (≈1.1nm) wide. For the plate simulations the x- and y- directions are periodic and the z-direction (thickness direction) is clad by a rigid (fixed) boundary (such as might be present as an oxide layer at the surface). Here the periodic plate width is 2 unit cells (≈1.1nm) and the z-direction thickness varies from 1 to 10 cells (≈0.54nm to 5.4nm). For the wire simulations the x-direction is periodic and the y- and z-directions have rigid boundaries. The wire is square in cross section and has a thickness varying from 1 to 10 cells (≈0.54nm to 5.4nm).

Particle velocities are distributed according to the Maxwell Boltzmann distribution corresponding to a finite but low temperature (1 K for the results presented in this study) as to activate incoherent particle vibrations with arbitrary spatial variation. The system is equilibrated for 100,000 time steps so that particle motion is no longer affected by the randomness of the initial velocity distribution and is instead governed by the normal vibrational modes of the structure.

After system equilibration, the system progresses for an additional 240,000 time steps and particle velocities are recorded every 10 time steps. After the full time history of particle velocities has been recorded, the spectral energy density method {13} is used to calculate the structure's x-direction dispersion relation. The spectral energy density is found by projecting velocities of the particles in the structure onto a generic form of a traveling wave characterized by x-direction wavenumber, k_x, and angular frequency, ω. The spectral energy density of a mode corresponding to a unique wavenumber and frequency is calculated using:

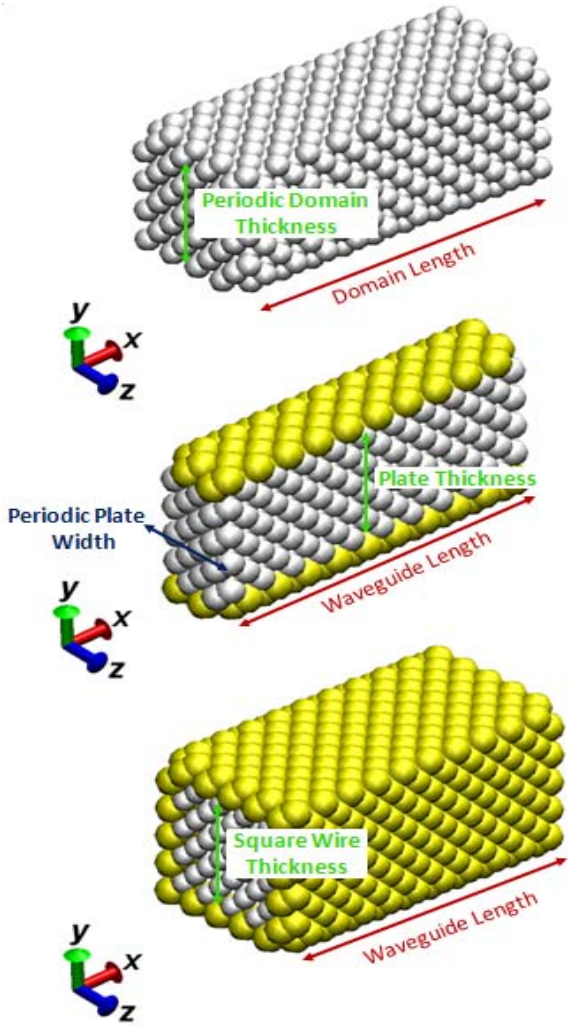

Figure 3: Illustration of Bulk (top), Thin Film 'Nanoplate' (middle) and Nanowire (bottom) Geometries

$$\Phi\left(k_x,\omega\right)=A\sum_{\alpha}\left|\int_0^{\tau_0}\sum_{j}^{N_a}\dot{u}_{j,\alpha}\left(t\right)\exp\left[ik_x x_{j,0}-i\omega t\right]dt\right|^2 \tag{4}$$

where $\dot{u}_{j,\alpha}\left(t\right)$ is the j[th] particle's velocity component in the α direction. The quantity A is a normalization constant that is not important for the calculation since only the *location* of spectral energy density peaks is required, not the magnitude. The peaks in the spectral energy density calculated at each x-direction wave number k_x constitute each wavenumber's possible frequencies of vibration. The amplitude of the peaks can then be plotted as a function of frequency and wavenumber and connected to form each branch of the nanostructure's dispersion relation.

3.2.3 Calculation of Transmission Function with Molecular Dynamics

Transmission functions are calculated in MD by generating a wave packet centered at frequency ω at the left end of the domain and calculating the fraction of total energy (kinetic + potential) that is transmitted as it propagates through the waveguide to the right end of the domain. Reference potential energies for transmission calculation are taken from the initial unexcited configuration. The wave packet is generated by driving a rigid wall on the side of the simulation domain, using an exponentially damped displacement of the form

$$x_j(t) = x_j(0) + U\sin[\omega(t - t_{center})]e^{-\eta^2(t-t_{center})^2} \quad (5)$$

where $x_j(t)$ denotes the position of atom j at time t. U, η, and t_{center} are packet amplitude, temporal decay parameter, and time of maximum displacement, respectively. Typical atomic displacements are 1% of the lattice parameter or lower in order to mimimize anharmonic packet distortion and thereby ensure linearly elastic wave behavior. The motion of the driven wall then creates a traveling wave packet in the material adjacent to the wall.

3.3 Continuum Approaches

3.3.1 Overview

Although continuum-based approaches are not able to handle high wavenumber/high frequency transport phenomena nor directly account for some nanoscale size effects, they are applicable in situations where long-wavelength, low frequency phonons dominate the thermal transport. Comparisons between continuum and MD methods were undertaken, for low frequency, long wavelength conditions, in order to provide validation of the new MD simulation models set up for the present project. Two types of continuum approaches were implemented: the superposition of partial waves analytical method and the finite difference time domain method.

3.3.2 Superposition of Partial Waves Method

The superposition of partial waves (SPW) method presented by Solie and Auld {14} is an analytical approach also used to calculate dispersion relations. There, the problem of the elastic plate with stress-free boundary conditions was solved for elastic wave propagation in cubic crystal systems where the axes of the plate are aligned with the material's crystal axes. Here, their solution method is modified to account for the displacement free boundary conditions. In the method, the Christoffel matrix equation is used to find the generic forms of the partial traveling elastic waves that are possible for the given crystal structure and orientation. The zero displacement boundary conditions are implemented to determine the magnitudes of the partial waves and to relate both the longitudinal and transverse components of wavenumber to the excitation frequency. For the case where the sagittal plane of the waveguide (x-z plane) is aligned with the cubic crystal axes, the theoretical displacement field under elastic wave propagation separates into three distinct mode families: shear horizontal modes (SH modes), symmetric Lamb modes (S modes), and antisymmetric Lamb modes (A modes). SH modes are uncoupled modes polarized only in the y-direction.

The calculations are performed on a single crystal silicon planar waveguide that extends infinitely in the x and y directions, and has finite width with fixed boundaries in the z-direction (Fig. 4). The x-axis is aligned with the [100] crystal direction. Particle displacement fields are assumed to be uniform in the y-direction so that only one direction (along the x-axis) of phonon propagation is considered. The plate boundaries at ±h/2 are fixed such that all components of displacement are zero. This geometry was chosen because it provides the closest correspondence to the MD simulations.

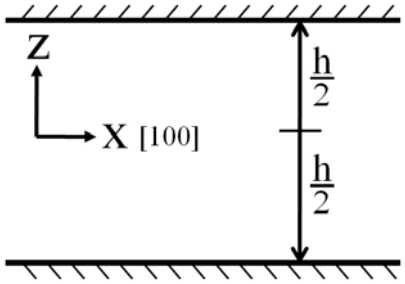

Figure 4: Idealized Geometry of Thin Film 'Nanoplate' Waveguide used in Superposition of Partial Waves Analysis

The calculations assume that the material is linearly elastic and anisotropic and that material parameters are constant with frequency and wavenumber. The elastic stiffness constants used in the calculations, c_{11}=150GPa, c_{12}=76GPa, and c_{44}=60GPa, are taken from a computational study of crystalline silicon approximated by the Stillinger-Weber potential.

3.3.3 Finite Difference Time Domain Method

The finite difference time domain (FDTD) technique is a numerical approach that solves an anisotropic linear wave equation in three dimensions using a series of discrete points in space and a set of finite difference approximations. It tracks displacement at nodes in a constructed grid. In the FDTD model, each region of space or set of similar nodes must be separately divided and assigned some stiffness values represented by a matrix $\bar{\bar{C}}$. While useful for macroscopic problems, this technique will not allow the user to easily incorporate spatial variations in $\bar{\bar{C}}$ that occur at length scales approaching atomic spacings. FDTD models can provide reasonable predictions at or above the micrometer scale and at wave numbers in the linear region of the dispersion relation (MHz-GHz range). In contrast to SPW, FDTD can treat anisotropic cases and complex waveguide geometries. However, the method is more computationally involved than SPW. FDTD calculations were run in their regimes of validity (at low frequencies and low wavenumbers) and compared to MD simulations in those regimes for additional validation.

4.0 RESULTS

4.1 Overview

Calculations were performed on bulk silicon and silicon nanostructures to validate the models, to investigate confinement effects on phonon dispersion relations, and to determine the effect of geometrical configuration on phonon transmission. Details of the results are described below.

4.2 Confinement Effects on Phonon Dispersion Relations

4.2.1 Validation of Phonon Dispersion Relation Calculations

Validation of the MD phonon dispersion relation calculations was performed by comparing MD dispersion relations for bulk Si and confined Si at low frequencies to those of other approaches. These approaches include experiments and lattice dynamic calculations done by other groups as well as SPW and FDTD modeling done in the present work.

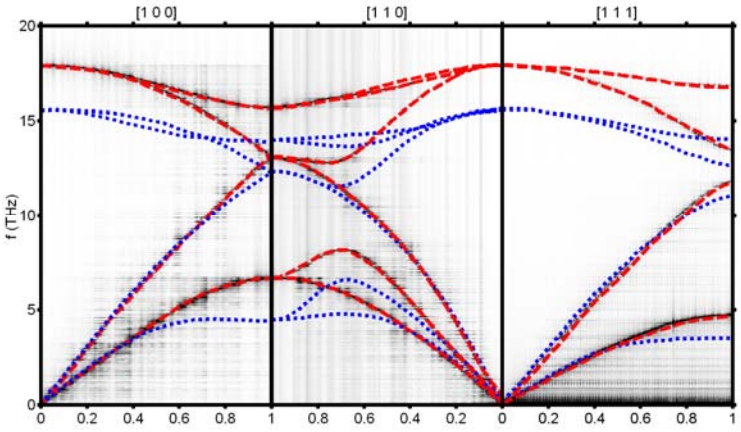

Figure 5: Dispersion Relation of Bulk Silicon calculated by Stillinger-Weber Lattice Dynamics (Red) {1}, Stillinger-Weber Molecular Dynamics (Black, Directly Behind Red Curve), and Experiment (Blue) {2}

For bulk Si, excellent quantitative agreement with the calculated dispersion relations of Jian et al. {1}, which were based on the Stillinger-Weber potential, was found (Figure 5). Comparison to the experimental data of Holt et al. {2} yields good quantitative agreement at most acoustic frequencies and qualitative agreement with optical branch frequencies. It should be noted that the Stillinger-Weber potential is known to overpredict optical phonon frequencies and some acoustic frequencies, hence the slight quantitative differences with experiments. Note that the horizontal axis is wavenumber normalized by $2\pi/a$, where a is the silicon lattice constant. For confined Si, validations were performed by calculating the dispersion relation of the lowest order S mode using SPW, FDTD, and MD methods. At low frequencies and for single mode excitations FDTD, MD, and SPW all agree very well (Fig. 6). This behavior is expected as the atomistic calculations approach the continuum limit in this regime. Note that the dimensionless frequency ω^* is equal to hw/V, where ω is frequency, h is the waveguide height and V is the shear wave velocity. The dimensionless wavenumber k^* is equal to kh, where k is wave vector and h is waveguide height. Material parameters used in the calculations were taken for Lennard-Jones argon.

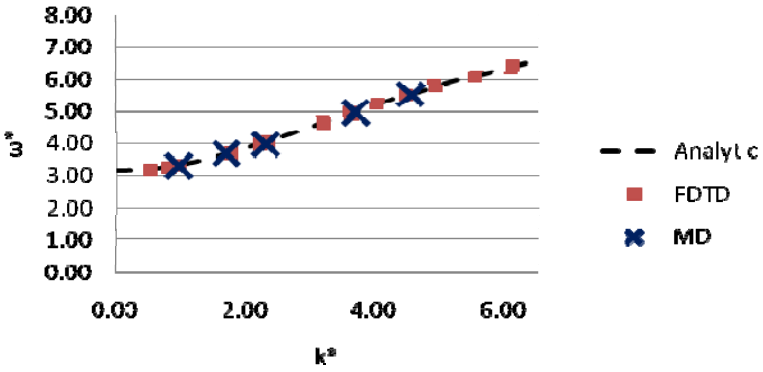

Figure 6: Dispersion Relation of Lowest Order Symmetric Model Silicon Thin Film Waveguide calculated by Superposition of Partial Waves ('Analytic'), Finite Difference Time Domain (FDTD), and Molecular Dynamics (MD)

4.2.2 'Nanoplate' Dispersion Relations

Once the validation calculations above were performed, a series of simulations on the thin film ('nanoplate') and nanowire geometries shown in Figure 3 were performed to examine the effects of size on the dispersion relations. The film thickness and square side length were the dimensions varied in the simulations. These dimensions are listed in terms of the number of unit cells that fit in the dimension of interest. 1 unit cell corresponds to 0.543 nm in physical length. Figure 7 illustrates the results for the nanoplate. For the thinnest plates, a clear nonzero minimum frequency is apparent in the dispersion. As thickness increases, the minimum frequency decreases. At a thickness of 40 unit cells (~ 22 nm), the minimum has decreased to about zero and a bulk-like spectrum begins to emerge. The implication of the nonzero minimum frequency is that a minimum thermal energy is required to excite phonon modes in very small nanostructures with rigid boundary conditions. At very low temperatures, few (or no) modes will be populated in confined structures as compared to bulk materials at the same temperature. For example, the 10 K temperatures of interest for infrared sensor cooling correspond to thermal energies with characteristic frequencies of 1.3 THz. Structures with minimum frequencies of this order and higher (e.g. the 1-4 cell thickness cases in Figure 7) will experience significant thermal conductivity reduction as there will be insufficient thermal energy to excite lattice vibrations.

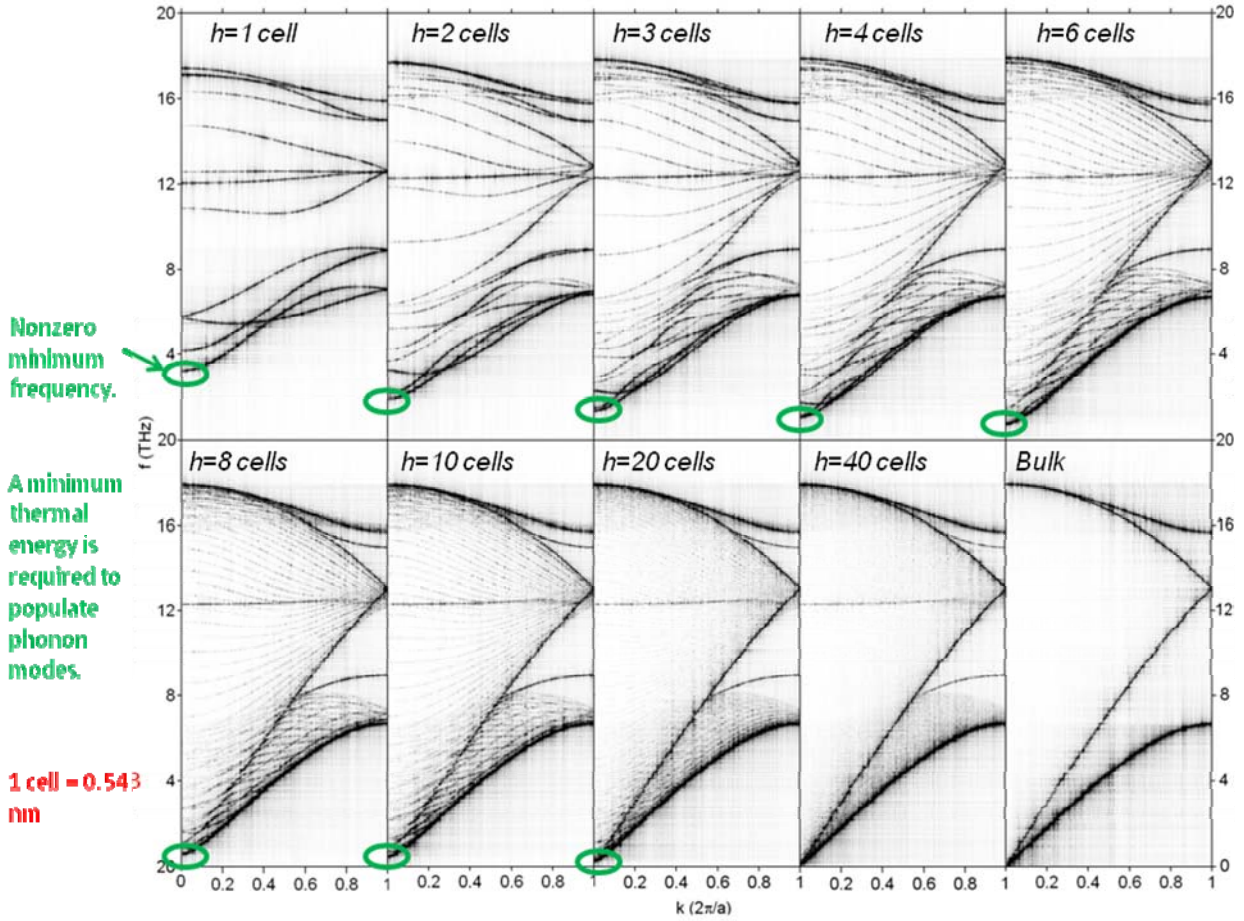

Figure 7: Confinement Effect on Dispersion Relations of Silicon 'Nanoplates'

Additionally, it should be noted that the smallest structures have several discrete 'branches' in the phonon dispersion relations that correspond to structural vibrational modes. As the size increases, these branches eventually collapse onto the longitudinal and transverse acoustic and optical phonon modes for bulk silicon. The slopes of most of the branches in the confined structures are flatter than those of the bulk case, which means that the phonon group velocities and ultimately thermal conductivities (see Equations (2) and (3)) will be smaller than for the bulk case. Another implication of the flat branches is that forbidden frequency gaps open up for the smallest nanostructure sizes, limiting the number of phonon frequencies that can participate in thermal conduction. The variation of dispersion relation with nanostructure size, both with regard to the minimum frequency and the flatter slope, indicates that the use of bulk dispersion relations for nanostructure thermal conductivity calculations is questionable.

4.2.3 Nanowire Dispersion Relations

Dispersion calculations were also performed for the nanowire geometry. Due to the two-dimensional confinement, the effects are even more pronounced than for the nanoplate case. A higher minimum frequency is observed for the smallest dimensions, and numerous flat branches are observed.

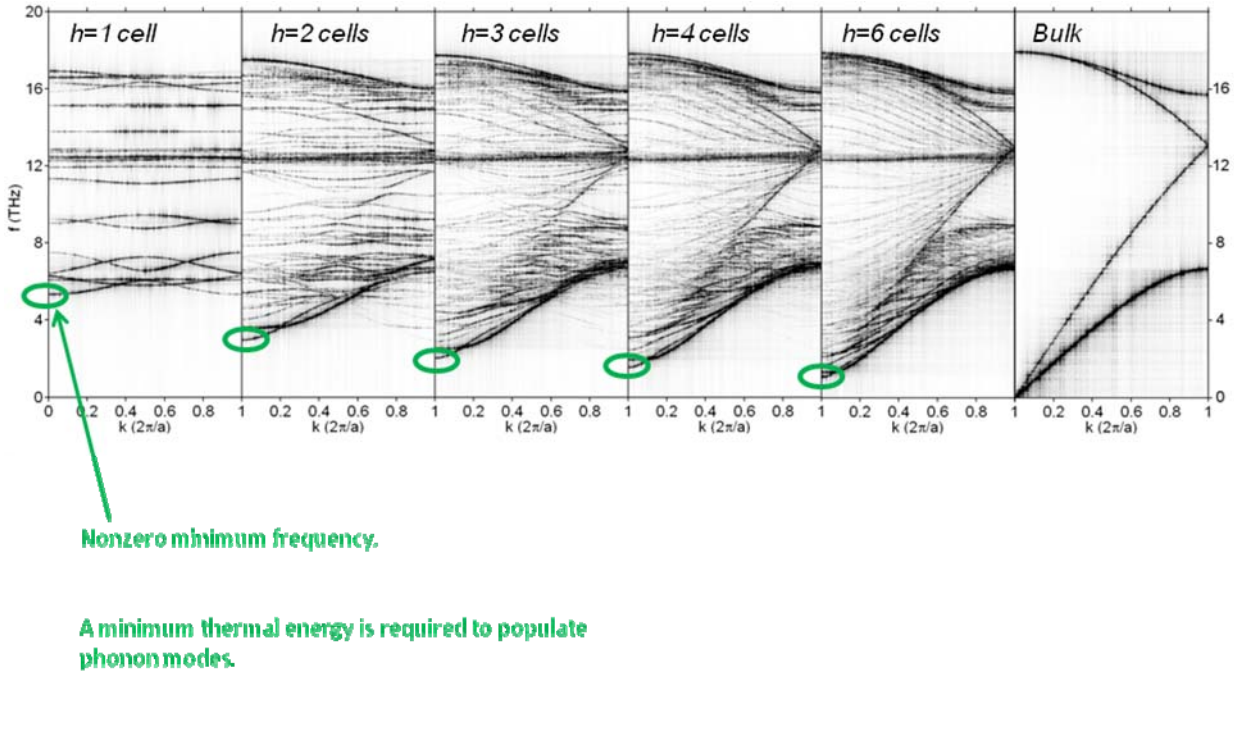

Figure 8: Confinement Effect on Dispersion Relations of Silicon Nanowires

4.3 Wall Geometry Effects on Phonon Transmission

4.3.1 Overview

From Equation (3), it is evident that the phonon transmission function should be mimimized over a broad range of phonon frequencies to minimize thermal conductivity. Calculations on nanoplate waveguides with various wall 'roughness' configurations were performed in order to elucidate the relationship between wall geometry and phonon transmission. Simple wall configurations were investigated in order to identify the key geometrical features affecting phonon transmission. Phonon transmission functions were calculated using MD and FDTD using the approach described in Section 4.2.3. To check the computational methods, calculations were performed on nanowires with perfectly smooth walls. Transmission functions with value 1 were computed for these cases. This value was expected, as there is negligible phonon-phonon scattering on the time scales measured and the featureless walls prevent backscattering.

For the simple geometries considered here, there are three important dimensions: nanoplate height, constriction height, and constriction length (Figure 9). The constriction provides a basic representation of the effect of roughness and is represented as a single aligned pair of asperities. Note that the white atoms represent the waveguide and the yellow atoms represent the fixed boundary. Only the white atoms are able to vibrate and carry the phonon wave packet. As described above, a wave packet is excited at the left boundary, traverses the waveguide until it encounters the constriction, and is partially reflected and partially transmitted through the asperity. The phonon transmission function represents the fraction of incident energy that is transmitted through the constriction.

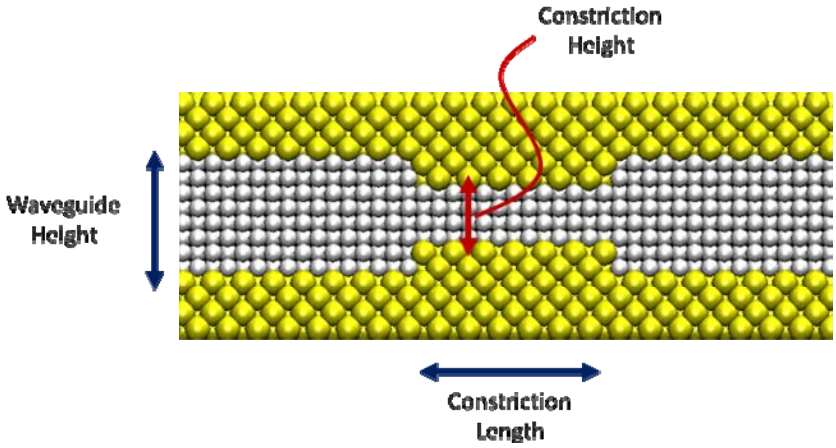

Figure 9: Illustration of Wall Roughness Geometry. Key dimensions: Overall Waveguide Height, Height of Constricted Portion of Waveguide, and Length of Constricted Portion of Waveguide

4.3.2 Single Constriction of Variable Height

The results of FDTD transmission calculations (performed in this instance on the standard benchmark material argon rather than for silicon) are shown in Figure 10 in terms of transmission function versus phonon frequency. The percentages in the figure indicate the constriction height compared to overall waveguide height, with smaller percentages representing the narrowest constrictions. The waveguide length for all cases shown in the figure is 2.4 nm. Transmission is observed to be zero below a minimum frequency for several of the constriction heights. This minimum frequency increases as the constriction becomes narrower. These results are consistent with the minimum frequencies observed in the dispersion relations above, and

provide another interpretation of why thermal conductivities are reduced in small nanostructures. An additional feature of Figure 10 is that peaks reminiscent of constructive interference fringes appear at various frequencies. This characteristic indicates that the wave nature of phonon transport is playing a role in phonon transmission through non-smooth waveguides and will ultimately affect the thermal conductivity of waveguide nanostructures.

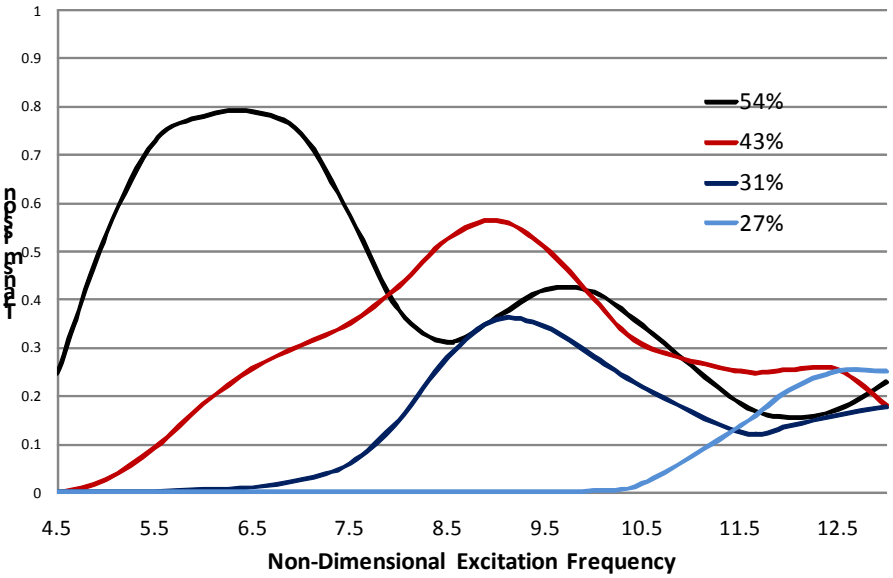

Figure 10: Wavepacket Transmission as a Function of Frequency for Single Constriction Waveguide for Various Constriction Heights. Percentages Indicate Constriction Height Compared to Overall Waveguide Height

4.3.3 Single Constriction of Variable Length

The results of MD transmission calculations (performed in this instance on the standard benchmark material argon rather than for silicon) are shown in Figure 11 in terms of transmission function versus phonon frequency. The symbols in the figure indicate the constriction length, with smaller values representing the shortest constrictions. For all cases shown in the figure the overall waveguide height is 2.4 nm and the constriction height is 1.3 nm. To first order, the results show similar transmission behavior at the various constriction lengths studied. The features common to all constriction

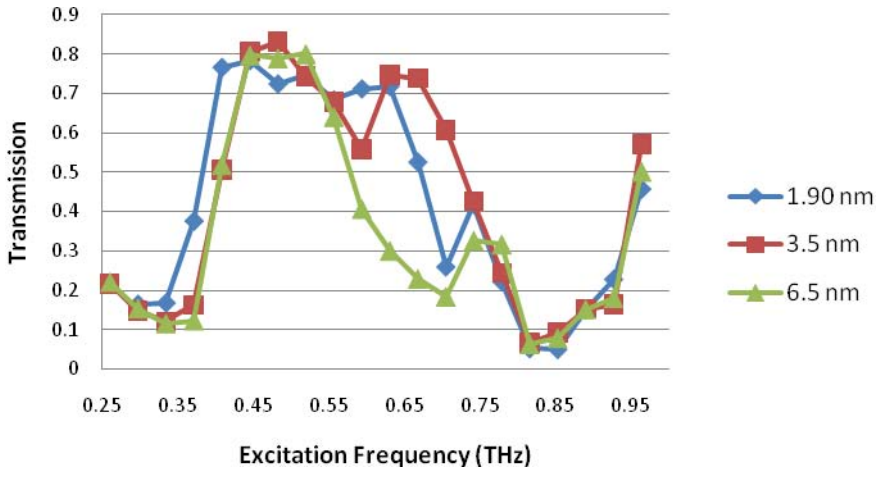

Figure 11: Wavepacket Transmission as a Function of Frequency for Single Constriction Waveguide for Various Constriction Lengths. Symbols Indicate Constriction Length

lengths are a broad plateau region at mid-range frequencies with higher transmission, with two 'sub-peaks' whose location varies with constriction length. Outside the plateau, the transmission exhibits a dip and then an increase as frequencies are either raised or lowered, and the values for all lengths exhibit the same transmission values. The peaks observed at the various frequencies are indicative of wave transport behavior.

4.3.4 Constriction with Sinusoidal Roughness of Variable Amplitude

FDTD simulations were performed to examine the effect of rough walls on waveguide. A sinusoidal roughness was added to the walls and the amplitude was varied to observe the effects. Fig. 12 shows that phonon transmission decreases strongly with amplitude. At the highest amplitudes phonon transmission is almost zero, indicating that very rough walls may be very effective at reducing thermal conductivity.

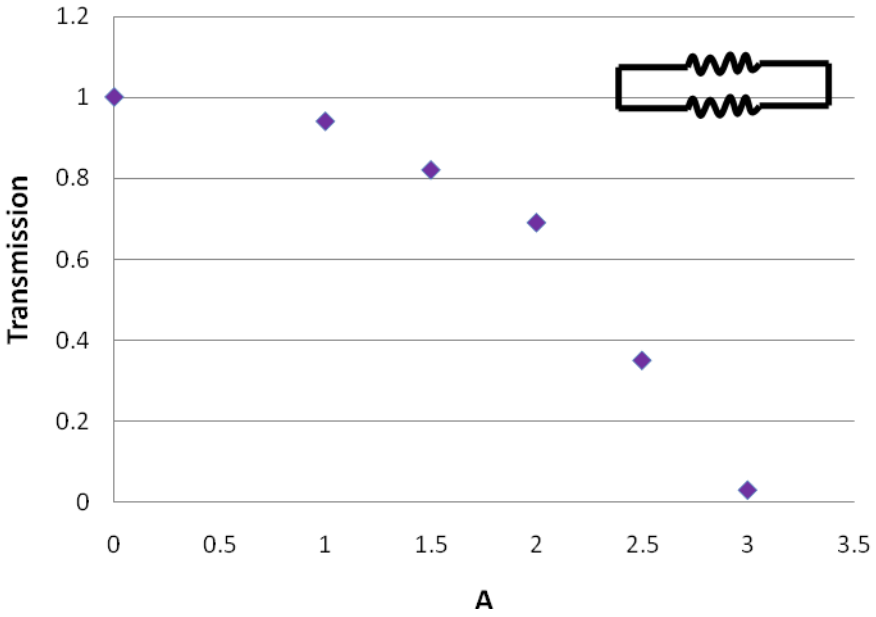

Figure 12: Wavepacket Transmission as a Function of Frequency Roughness Amplitude

5.0 SUMMARY AND CONCLUSIONS

5.1 Overview

Phonon dispersion relations and transmission functions were calculated for nanoscale thin films and nanowires of different geometrical configurations using molecular dynamics and finite difference time domain simulations. These two parameters are critically important in understanding how thermal conductivity can be reduced by tailoring the geometry and dimensions of such structures.

5.2 Dispersion Relation Results

The dispersion relation calculations were validated against known bulk material dispersions to test the calculation approach and good agreement was found. For small nanostructures, confinement was found to dramatically change the dispersion relation in ways that reduce

thermal conductivity. These include widely spaced bands, which means that fewer bands exist at the low frequencies of interest for low temperature thermoelectrics, and flatter dispersion relations, which lead to a reduction in phonon velocity. Importantly, a minimum frequency that increases with decreasing nanostructure size was observed. For very small nanostructures, the minimum frequency was found to be larger than that associated with thermal phonons at 10 K. The implication of this result is that the thermal energy at these temperatures is not sufficient to populate the bands, and that very low thermal conductivity is expected as a result.

5.3 Transmission Results

Simple nanowire geometries were investigated to observe the effects of geometrical configuration on phonon transmission. The reduction of phonon transmission is desirable as this leads to thermal conductivity reduction. Specifically, nanowires with constrictions of varying length and width were investigated, and nanowires with sinusoidal 'rough' walls were investigated. In all cases, the appearance of peaks at different frequencies shows that our modeling approaches capture wave behavior. Narrowing the constriction was found to have a more prominent effect on reducing phonon transmission than lengthening the constriction. Rough wires showed a dramatic reduction in transmission as roughness amplitude was increased.

6.0 RECOMMENDATIONS FOR FUTURE WORK

Several recommendations for thermal conductivity reduction emerge from the above preliminary studies. First, comprehensive studies to identify the direct relationship between geometrical feature size and thermal conductivity reduction are recommended. Such studies will provide guidelines for the exact geometrical dimensions needed to fabricate low thermal conductivity nanoscale thermoelectric materials for operation in a 10 K environment. The calculations described above, which are based on phonon *frequency*, provide this information in an aggregated way across multiple phonon branches but do not explicitly indicate the exact structure and dimensions needed to minimize phonon transmission. Calculations based on wavelength/wavevector, because they specifically are related to a physical length, are expected to provide this information. Relevant examples include the tuning of superlattice structures and of layered thin film antireflective coatings to optimize the reflection of phonons and photons of specific wavelengths. Toward this end, theoretical methods to calculate transmission of specific phonon modes as a function of wavelength/wavevector should be developed and used to identify the most promising structures for reduction of phonon transport. With this foundation, it is recommended that geometry and roughness tuning be applied to materials and structures promising for thermoelectric applications, including $FeSb_2$, Type II superlattices, and, potentially, nanocrystal superlattices. It is also recommended that experiments on the most promising structures identified in the calculations be performed to provide definitive evidence that thermal conductivity has been minimized in such structures.

BIBLIOGRAPHY

Allen, M. P., and Tildesley, D. J., **Computer Simulation of Liquids**, Clarendon Press, Oxford, 1987.

Dresselhaus, M. S., et al., "New Directions for Low-Dimensional Thermoelectric Materials," *Advanced Materials*, **19**, 2007, pp. 1043-1053.

Hochbaum, A. I., et al., "Enhanced Thermoelectric Performance of Rough Silicon Nanowires," *Nature*, **451**, 2008, pp. 163-168.

Holt, M., et al., "Determination of Phonon Dispersions from X-Ray Transmission Scattering: The Example of Silicon," *Physical Review Letters*, **83**, 1999, pp. 3317–3319.

Jian, Z., Kaiming, Z., and Xide, X., "Modification of Stillinger-Weber Potentials for Si and Ge," *Journal of Applied Physics*, **41**, 1963, p. 12915.

Joshi, G., et al., "Enhanced Thermoelectric Figure-of-Merit in Nanostructured P-Type Silicon Germanium Bulk Alloys," *Nano Letters*, **8**, 2008, pp. 4670-4674.

Kim, W., et al., "Thermal Conductivity Reduction and Thermoelectric Figure of Merit Increase by Embedding Nanoparticles in Crystalline Semiconductors," *Physical Review Letters*, **96**, 2006, p. 045901.

Mingo, N., "Calculation of Si Nanowire Thermal Conductivity Using Complete Phonon Dispersion Relations," *Physical Review B*, **68**, 2003, p. 113308.

Poudel, B., et al., "High Thermoelectric Performance of Nanostructured Bismuth Antimony Telluride Bulk Alloys," *Science*, **320**, 2008, pp. 634-638.

Stillinger, F. H., and Weber, T. A., "Computer Simulation of Local Order in Condensed Phases of Silicon," *Physical Review B*, **31**, 1985, pp. 5262-5271.

Solie, L. P., and Auld, B. A., "Elastic Waves in Free Anisotropic Plates," *The Journal of the Acoustical Society of America*, **54**, 1973, p. 50.

Thomas, J. A., Turney, J. E., Iutzi, R. M., Amon, C. H., and McGaughey, A. J. H., "Predicting Phonon Dispersion Relations and Lifetimes from the Spectral Energy Density," *Physical Review B*, **81**, 2010, p. 081411.

Tomlinson, B. J., Flake, B., and Roberts, T. (2002), "Air Force Research Laboratory Space Cryogenic Technology Research Initiatives," in *Cryocoolers 12*, ed. R. G. Ross Jr., New York: Springer, pp. 9-16.

Wang, X. W., et al., "Enhanced Thermoelectric Figure of Merit in Nanostructured N-Type Silicon Germanium Bulk Alloy," *Applied Physics Letters*, **93**, 2008, p. 193121.

DISTRIBUTION LIST

DTIC/OCP
8725 John J. Kingman Rd, Suite 0944
Ft Belvoir, VA 22060-6218 1 cy

AFRL/RVIL
Kirtland AFB, NM 87117-5776 2 cys

Official Record Copy
AFRL/RVSE/Keith Avery 1 cy

(This page intentionally left blank)